Berliner Beiträge zur Archäometrie, Kunsttechnologie und Konservierungswissenschaft

Band 23

Berlin 2015

Rathgen-Forschungslabor
Staatliche Museen zu Berlin

Herausgeberin:
Dr. habil. Ina Reiche
Rathgen-Forschungslabor, Staatliche Museen zu Berlin –
Stiftung Preußischer Kulturbesitz
Schloßstraße 1 a
14059 Berlin

Redaktionsassistentin:
Sabrina Buchhorn
Rathgen-Forschungslabor, Staatliche Museen zu Berlin –
Stiftung Preußischer Kulturbesitz

Herstellung:
Buch- und Offsetdruckerei H. Heenemann GmbH & Co. KG
Bessemerstraße 83 – 91
12103 Berlin
Printed in Germany

ISSN: 0344-5089

Inhalt

Scanning macro-X-ray fluorescence analysis and Neutron Activation Auto Radiography: Complimentary imaging methods for the investigation of historical paintings

Matthias Alfeld[1,2], Claudia Laurenze-Landsberg[3], Andrea Denker[4], Koen Janssens[2] and Petria Noble[5]

[1] Laboratoire d'Archéologie Moléculaire et Structurale (LAMS), UMR 8220/Université Pierre et Marie Curie/Paris 6, Sorbonne Universités, 4 place Jussieu, BC 225, 75005 Paris, France
[2] University of Antwerp, Groenenborgerlaan 171, 2020 Antwerp, Belgium
[3] Gemäldegalerie Berlin, Stauffenbergstraße 40, 10785 Berlin, Germany
[4] Helmholtz-Zentrum Berlin für Materialien und Energie (formerly Hahn-Meitner-Institute), Hahn-Meitner-Platz 1, 14109 Berlin, Germany
[5] Rijksmuseum, Museumstraat 1, 1070 DN Amsterdam, The Netherlands

Abstract

The last years have seen an impressive development in the field of imaging techniques for the study of historical paintings. One of the most crucial developments is that of scanning macro-X-ray fluorescence analysis (MA-XRF), which allows for the acquisition of elemental distribution images of entire paintings, without removing the painting from the museum or gallery it is exhibited in. Another imaging technique, Neutron Activation Auto Radiography (NAAR) is known since the 1960s and allows for the acquisition of images with elemental contrast, but has the disadvantage that it requires the transport of the painting to a research reactor, where it has to stay for several weeks.

In this paper we compare the results of both techniques in a study of *Adoration by the Shepherds* by Pieter Cornelisz van Rijk (1568 – 1628). It will be shown that XRF imaging is faster, easier to realize, sensitive to a wider range of elements and provides images that are easier to interpret. However, NAAR can provide information on layers that cannot be investigated by XRF as the more energetic β-radiation is less hindered by absorption effects in covering layers, than the comparatively lower energetic photons detected in XRF.

1 Introduction

Historical paintings are investigated by scientific methods to gain insight in their creation process, to visualize overpainted works and to support their preservation for coming generations (Alfeld & Broekaert, 2013). Imaging methods providing visual representations with limited or no chemical or elemental contrast are traditionally employed along with spectroscopic spot analysis methods. The most prominent ones are X-ray radiography (XRR) and Infrared Reflectography (IRR). In XRR, the intensity of X-rays transmitting through the painting is recorded by a photographic medium, so that less absorbing areas appear dark on the image (Bridgman, 1964).

In IRR the intensity of IR radiation from flash lights reflected, i.e. not absorbed, by the painting is measured. One of its main features is that it reveals the distribution of the strongly IR absorbing black carbon based pigments, which was often used for preliminary sketching (van Asperen de Boer, 1968). Beyond that, spectroscopic methods, such as X-ray fluorescence analysis (XRF) are used to gain insight in the elements present. Here a small area is excited with a focused or collimated beam and the emitted fluorescence radiation is recorded in an energy dispersive fashion (Snickt et al., 2010). In the thus obtained spectra the elements present are identified by their fluorescence signals. While XRF can detect all elements heavier than Na (Z=11), in practice it suffers from absorption effects between sample and detector. Only elements heavier than S (Z = 16) can be well detected in surface layers. In layers under the surface of a painting only those elements heavier than Cu (Z = 29) can be reliably detected.

The last years have seen a rapid development of imaging techniques. A multi- or hyperspectral component has been added by the introduction of energy or wavelength dispersive detection, which makes it possible to distinguish between different elements or chemical components (Delaney et al., 2010; Cabal et al., 2015). The spot investigation technique XRF was extended to scanning macro-XRF (MA-XRF) by scanning the surface and acquiring images pixel by pixel. In the acquired elemental distribution images the greyscale represents the relative intensity of the respective fluorescence line. To facilitate an easier comparison of images, in this publication the colour scale is set so that the most intense pixels are shown as black, while those pixels with the least intense signal are shown as white. While the first MA-XRF experiments were done at synchrotron sources (Dik et al., 2008), quickly mobile, X-ray tube based instruments became available (Alfeld et al., 2011) allowing for in-situ investigations of paintings in museums and galleries. The ease of application and the relative fast measurements

Figure 1: Pieter Cornelisz van Rijk, *Adoration by the Shepherds*, ca. 1615, oil on canvas on panel, 23.0 × 31.5 cm (Gemäldegalerie Berlin, Catalogue Number 1498), normal light photograph (left) and XRR (right). In the radiograph less X-ray absorbing areas are indicated by a darker shade.

have established MA-XRF in the last years as a method for the investigation of historical paintings, with commercial instruments being available (Alfeld et al., 2013a). Next to imaging, XRF also allows for depth profiling by utilizing a confocal geometry. Here a focused beam is used and the field of view of the detector is limited by the installation of a second focussing optic, so that only fluorescence radiation from a small volume of a few tens of micrometer diameter is detected. By moving the sample through this volume depth profiles are obtained. The technique was first described for historical paintings in 2003 (Kanngießer et al., 2003) and its application is continued in the present days (Reiche et al., 2012).

These developments notwithstanding, already since the 1960s a technique that combined imaging with elemental contrast has been available: Neutron Activation Auto Radiography (NAAR) (Sayre & Lechtman, 1968). Here short-term radioactivity is induced in the painting by thermal or cold neutrons from a research reactor and the emitted β-radiation is recorded with a photographic medium. While this detection is neither energy nor wavelength dispersive, elemental contrast can be achieved by exploiting differences in the half-lives of the created radio-nuclides. As a result, the relative intensity of the emitted β-radiation of different radio-isotopes varies with time. Long living radio-isotopes are best detected when the more short-lived ones have faded, while the latter are best detected directly after activation when the relative intensity of their β-radiation is highest. In this technique a darkening of the film indicates the presence of one or several of the contributing radio-isotopes. While one cannot directly identify the radio-isotope giving rise to the darkening, it can be interfered by comparing the autoradiographs with one another, the visual image of the painting and spot analysis techniques. An example for the latter is energy dispersive spectroscopy of the γ-radiation emitted by the painting after activation.

Given the differences in the physical process generating the radiation, its nature and its detection, a theoretical comparison between MA-XRF and NAAR is not straightforward. Also, in many cases it is not advisable to expose a historical painting to the stress of scientific investigation for the sake of comparing imaging techniques. On the other hand, the investigation of test samples does not always provide satisfying answers, as they often fail to reproduce the complexity of an actual historical painting.

Recently, Seim et al. used NAAR and XRF for the investigation of *The Reading Hermit* allegedly painted by Rembrandt, but the art-historical findings were more the focus of their work, than a comparison of methods (Seim et al., 2014).

The authors of this study have compared both imaging techniques on Rembrandt's *Susanna and the Elders* (Alfeld et al., 2015). In the framework of these experiments also *Adoration by the Shepherds*, by Pieter Cornelisz van Rijk (Delft, 1568 – 1628) was investigated (s. Figure 1). The painting is of little art-historical interest, but was used by C.O. Fischer et al. in a metrological study on NAAR (Fischer et al., 1987), not the least because it features a wide range of typical 17th century pigments. During their investigation they also detected paint layers not belonging to the final painting, but to part of an underlying composition, on top of which *Adoration by the Shepherds* was painted. In this paper we compare the XRF results obtained on this painting with the autoradiographs acquired by Fischer, which complement the results of our earlier published work.

While the NAAR investigation of the panel was done at the Institute Laue-Langevin (ILL) in Grenoble, France, the experience gained during these experiments contributed to the investigation of further paintings at the BER II research reactor at the Helmholtz-Zentrum Berlin (formerly the Hahn-Meitner Institute).

The painting is executed on a piece of canvas glued on a wooden support. It shows a group of shepherds, which arrive at the stable shortly after the birth of Jesus and their adoration of the new born child. A group of persons is positioned inside or in front of a stable, next to which a small tree in growing. Besides the group around the child, the painting features a man making a fire in the lower right corner and some animals. The background of the painting features a blue sky and a green landscape.

Figure 2: "Instrument D" during the investigation of *Adoration by the Shepherds* in the photography studio of the Gemäldegalerie Berlin (DE).

The X-ray radiograph of the painting (s. Figure 1) is dominated by the distribution of lead in the painting. As the ground layers of the painting presumably contained this element, the extend of the original canvas is easily discernible. In the central lower part of the painting a slightly tilted square can be seen, which has no correlation with a visible feature of the painting and might be part of a hidden composition.

2 Experimental

2.1 MA-XRF

The painting was investigated by means of an in-house built scanner of the University of Antwerp named "Instrument D" (s. Figure 2). The instrument, whose complete characterization is published elsewhere (Alfeld et al., 2013b), consists of a measurement head, which is mounted on a XY motorized stage (Newport Corporation, Irvine, CA, USA) with 60 cm travel range in both directions. The measurement head consists of a 10 W Rh-anode transmission X-ray tube (Moxtek, UT, USA) and four detectors. The primary beam is defined by a Pb collimator with a diameter of 0.8 mm, yielding a beam slightly larger than 1 mm on the surface of the painting. As detectors four Silicon Drift (SD-)detectors (two Vortex EX-60 and two Vortex EX-90, SII, Northridge, CA, USA) were used.

The analogue signals obtained from the detectors' preamplifiers were processed in a DXP-XMAP (XIA LLC, Hayward CA, USA). The primary beam impinged on the surface of the painting at normal angle and was detected under approx. 45 degrees.

The painting was scanned with a step size of 1 mm (vertical) and 0.5 mm (horizontal) and a dwell time of 0.15 s per pixel. Consequently the scan took a little less than six hours. The images shown were interpolated to a pixel size of 0.5 mm × 0.5 mm.

From the raw spectral data the signal intensities of the elements were calculated and elemental distribution images produced by dedicated software packages: Datamuncher (Alfeld & Janssens, 2015) and PyMCA (Solé et al., 2007). Contrast and dynamic range of all images were adjusted for best readability.

2.2 NAAR

The NAAR experiments were carried out at the neutron guide SN7 of the Institute Laue-Langevin (ILL) in Grenoble, France, using cold neutrons with an average wavelength of 0.45 nm and an average flux of 2.5×10^9 cm^{-2}/s. The neutron guide had a diameter of 3 cm × 5 cm (hor. × ver.). The neutrons impinged on the surface of the painting at an angle of 5.75°, so that a stripe of 5 cm × 31.5 cm was activated at a time. To achieve homogeneous activation of the entire surface, the painting was moved up and down through the neutron beam with 3.6 cm/min for four hours.

The three autoradiographs discussed in this work show the distribution of the following isotopes (half-lives in brackets): ^{56}Mn (2.6 h), ^{64}Cu (12.8 h), ^{76}As (26.4 h), ^{32}P (14.3 days), ^{203}Hg (46.6 days), ^{60}Co (5.3 years). The time windows of the autoradiographs are given in Table 1. A full description of the experiment and the calculation of exposure times can be found in the original publication (Fischer et al., 1987).

3 Results and discussion

In Figure 3, autoradiographs 1 and 2 demonstrate the distribution of the elements, Mn, Cu and As. Mn is present in the dark earth pigment umber, which was used to model the roof of the stable, the coat of the central man and the shadows. Cu is present in unidentified blue and/or green pigments in the garments, the green landscape and the tree. As is present as a minor element in smalt, a finely ground Co-containing K-rich grey/ blue glass, which, depending on the Co ore and manufacturing process, contains notable amounts of other elements (Robinet et al., 2011).

The blue smalt was mainly used to colour the sky. While all three elements contribute to autoradiograph 1, they do not so equally. Cu causes the most intense darkening, followed by Mn, while the contribution of As is only faint.

In the second autoradiograph Mn has completely faded, so that only Cu and As contribute to blackening of the image. Also the ratio of these elements has shifted, with the slower decaying As having now a stronger relative contribution. This autoradiograph shows the same features as the first one, with one addition: with the Mn no longer contributing, in the centre of the painting a shape not visible in the composition can be discerned. This

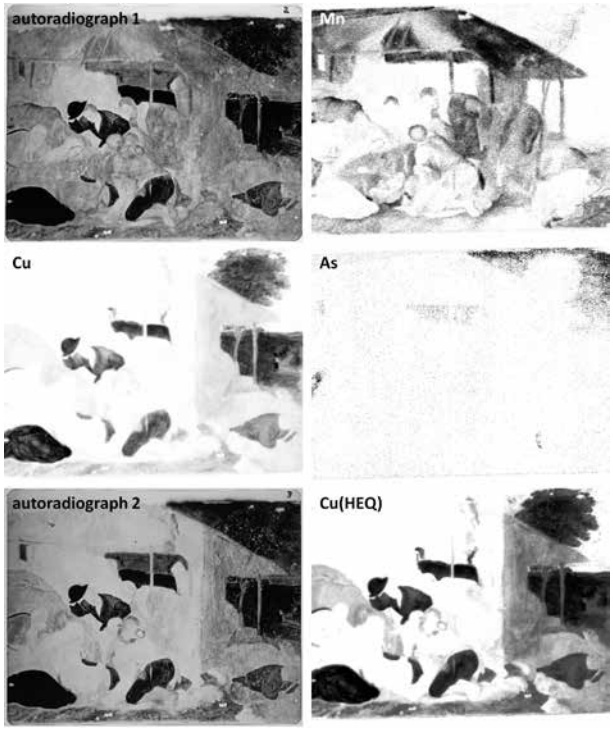

Figure 3: Autoradiographs 1 and 2 and elemental distribution images of Mn, Cu and As. Histogram Equalisation was used to adjust the contrast in the image labelled Cu(HEQ) to highlight the feature visible in the centre of the second radiograph. In all images a darker shade indicates a stronger signal.

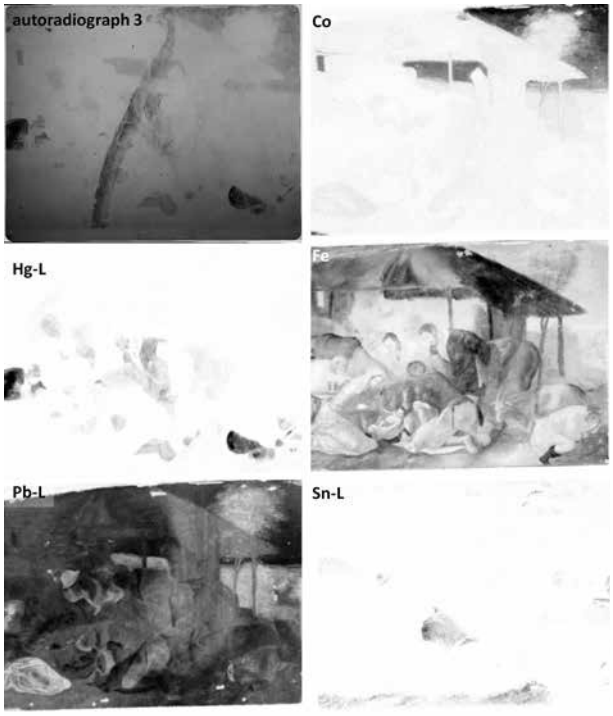

Figure 4: Autoradiograph 3 and elemental distribution images of Co, Hg, Fe, Pb and Sn. Sn, Hg and Pb were detected by their L-level fluorescence radiation. In all images a darker shade indicates a stronger signal.

Table 1: Time windows and contributing radio-isotopes of the three autoradiographs shown.

No. Autoradiograph	Time after activation	Duration	Contributing isotopes
1	0.5 hours	3 hours	^{56}Mn, ^{64}Cu, ^{76}As
2	15 hours	24 hours	^{64}Cu, ^{76}As
3	8 days	16 days	^{32}P, ^{60}Co, ^{203}Hg

shape is only faintly visible in the Cu distribution image, as its contribution is rather weak. If the colour scale of the image is adjusted by histogram equalization (Cu(HEQ)), the shape can be clearly seen, but might otherwise be easily missed. The better visualization of this feature in NAAR is mostly due to the fact, that the β-radiation emitted by ^{64}Cu is less strongly absorbed by covering paint layers than the Cu K-fluorescence radiation, which makes MA-XRF considerably more surface sensitive.

When comparing autoradiograph 2 and the Cu distribution image it can also be seen that the former features a much higher lateral resolution. Details in the paint application are simply lost in the elemental distribution images acquired by XRF.

In Figure 4, autoradiograph 3 several elemental distribution images are shown. The radio-isotopes of the elements P, Co and Hg contribute to this autoradiograph. Co, as discussed above, is present in the pigment smalt, which is used to paint the sky. Hg is present in the red pigment vermilion, used extensively in the red garments of the two persons and to model the flesh tones and garment in the centre of the painting. Both distributions are also clearly visible in the autoradiograph.

In addition to these contributions, also a large streak is visible in the autoradiograph, running slightly obliquely through the painting. This shape results from the distribution of P in bone black and belongs to the overpainted composition.

The detection of P by XRF is limited to surface layers due to the strong absorption of its low energetic fluorescence radiation. Since the detector electronics of the XRF scanner were optimized during the experiment for high count rates in the energy range above 3 keV, meant that P could not be detected. However, even with different detection settings, the streak would not be detected as it is below the surface and therefore not detectable by XRF.

In addition to the elements contributing to autoradiograph 3, the images of Fe, Pb and Sn are also shown, which cannot be detected by NAAR. Fe is present throughout the painting in the form of brown and red earth pigments, which were used to model, among other features, the garments, hair, the roof of the stable and the trunk of the tree in the background.

Sn is assumed to be present in lead tin yellow, which was used mainly in the yellow shirt of the kneeling man in the centre of the painting. In other areas, such as in the

ground below the central group, the green details on the landscape to the right and in the tree and the highlight on the hat of the man standing above Jesus, lead tin yellow was added to a Cu pigment to give it a brighter, more lively tone and for the highlights.

Pb is mainly present in lead white, which was used throughout the painting, and to a lesser degree in lead tin yellow. Yet, the latter contributes less to the Pb distribution image, as it was used only in relatively small amounts. It was stated that the radiograph (Figure 1) mainly represents the distribution of Pb. This is true when comparing the right part of both images, keeping the difference in contrast in mind. Here the roof of the stable is clearly distinct from the Pb-rich sky. In the left part of the painting areas with low Pb signals are visible that are nevertheless strongly absorbing, as seen in the X-ray radiograph. These are areas in which thick layers of Cu-containing paint were applied, that on the one hand prevent the detection of Pb radiation from the ground layers and on the other hand absorb the transmitted X-rays during the acquisition of the radiograph.

The elemental distribution images of Pb acquired in reflection geometry are in general more surface sensitive than X-ray radiographs acquired in transmission. While this means deeper, covered layers are more difficult to detect, it also reduces the contributions of ground layers and support, so that a more readable image is obtained.

Another element that is detectable by XRF but not by NAAR is Ca, the other element associated with bone black. The distribution map is not shown here. Its detection is limited to the surface of the painting.

It is not known from which painting the re-used canvas of *Adoration by the Shepherds* comes from and its composition is difficult to interpret from the few features visible in the autoradiographs. However, it is possible that the odd streak visible in autoradiograph 3 was the edge of a woman's décolleté and that the Cu-containing feature is a form of pendant. This becomes visible if we turn the painting by 90 degrees with the head of the sitter to the left of the composition of *Adoration by the Shepherds.*

4 Conclusion

It was shown that both techniques, MA-XRF and NAAR, are capable of visualizing the distribution of elements within the paint layers of *Adoration by the Shepherds.* MA-XRF was capable of detecting a wider range of elements, including Ca, Fe, Sn and Pb that are not detectable by NAAR, and provides images in which the contribution of different elements are clearly separated. Consequently, these images are easier to interpret by non-experts. Also the MA-XRF investigation was done in a single afternoon and did not require the transport of the painting to an external laboratory.

In these experiments the lateral resolution of the elemental distribution images acquired by MA-XRF was considerably worse than that of the autoradiographs. This is mainly due to the short time available for the experiment. Modern X-ray optics allow focusing of polychromatic beams of X-ray tubes to a few tens of micrometers and with these devices a lateral resolution in the same length scale might be achieved at the price of longer acquisition times. To acquire an image of the *Adoration by the Shepherds* with a pixel size of 50 µm with a dwell time of 10 ms per pixel the painting would be scanned for 73 hours or 3 days. Yet, this effort would only be justified for objects of high interest. In most cases areas of interest would be re-visited after a quicker overview scan with inferior lateral resolution.

The lateral resolution of NAAR is not dependent on the acquisition time, but on the photographic medium, the distance between photographic medium and the painting's surface and the energy of the emitted β-radiation. In the case of the digital reproductions of the autoradiographs acquired from *Adoration by the Shepherds* used in this work the lateral resolution achieved was estimated from details to be in the range of a 100 to 200 micrometer. However, the entire surface of the painting is depicted at the same lateral resolution.

The features of the overpainted work were only weakly (the Cu pendant?) or not at all visible (the P containing streak in autoradiograph 3), due to the absorption of radiation in covering paint layers. This is a fundamental difference in the methods, which will not be overcome by scientific developments in the future.

So, while MA-XRF is easier to use and interpret and allows for the detection of more elements, NAAR provides for a limited set of elements detection in deeper layers of the painting, which would otherwise remain undetectable, making both methods complimentary techniques for the scientific study of paintings.

5 Acknowledgements

This research was supported by the Interuniversity Attraction Poles Programme – Belgian Science Policy (IUAP VI/16). The text also presents the results of GOA "XANES meets ELNES" (Research Fund University of Antwerp, Belgium) and from FWO (Brussels, Belgium) Project Nos. G.0704.08 and G.01769.09. M. Alfeld received from 2009 to 2013 a PhD fellowship of the Research Foundation-Flanders (FWO).

References

Alfeld, M. & Broekaert, J. A. C. (2013): *Spectrochim. Acta, Part B*. 88, 211 – 230.

Alfeld, M. & Janssens, K. (2015): *J. Anal. At. Spectrom.* 30, 777 – 789.

Alfeld, M., Janssens, K., Dik, J., De Nolf, W., & Van der Snickt, G. (2011): *J. Anal. At. Spectrom.* 26, 899 – 909.

Alfeld, M., Laurenze-Landsberg, C., Denker, A., Janssens, K., & Noble, P. (2015): *Appl. Phys. A*. 119, 795 – 805.

Alfeld, M., Pedroso, J. V., van Eikema Hommes, M., Van der Snickt, G., Tauber, G., Blaas, J., Haschke, M., Erler, K., Dik, J., & Janssens, K. (2013a): *J. Anal. At. Spectrom.* 28, 760 – 767.

Alfeld, M., Van der Snickt, G., Vanmeert, F., Janssens, K., Dik, J., Appel, K., van der Loeff, L., Chavannes, M., Meedendorp, T., & Hendriks, E. (2013b): *Appl. Phys. A*. 111, 165 – 175.

Bridgman, C. F. (1964): *Stud. Conserv.* 9, 135 – 139.

Cabal, A., Schalm, O., Eyskens, P., Willems, P., Harth, A., & Van Espen, P. (2015): *X-Ray Spectrom.* 44, 141 – 148.

Delaney, J., Zeibel, J., Thoury, M., Littleton, R., Palmer, M., Morales, K., de la Rie, E., & Hoenigswald, A. (2010): *Appl. Spectrosc.* 64, 584 – 594.

Dik, J., Janssens, K., Van der Snickt, G., van der Loeff, L., Rickers, K., & Cotte, M. (2008): *Anal. Chem.* 80, 6436 – 6442.

Fischer, C. O., Kelch, J., Laurenze, C., Leuther, W., & Slusallek, K. (1987): *Kerntechnik*. 51, 9 – 13.

Kanngießer, B., Malzer, W., & Reiche, I. (2003): *Nucl. Instrum. Methods Phys. Res., Sect. B* 211, 259 – 264.

Robinet, L., Spring, M., Pagès-Camagna, S., Vantelon, D., & Trcera, N. (2011): *Anal. Chem.* 83, 5145 – 5152.

Reiche, I., Müller, K., Eveno, M., Itie, E., Menu, M. (2012): *J. Anal. At. Spectrom.* 27, 1715 – 1724.

Sayre, E. V. & Lechtman, H. N. (1968): *Stud. Conserv.* 13, 161 – 185.

Seim, C., Laurenze-Landsberg, C., Schröder-Smeibidl, B., Mantouvalou, I., de Boer, C., & Kanngießer, B. (2014): *J. Anal. At. Spectrom.* 29, 1354.

Solé, V. A., Papillon, E., Cotte, M., Walter, P., & Susini, J. (2007) : *Spectrochim. Acta, Part B*. 62, 63 – 68.

Van Asperen de Boer, J. R. J. (1968): *Appl. Opt.* 7, 1711 – 1714.

Van der Snickt, G., Janssens, K., Schalm, O., Aibéo, C., Kloust, H., & Alfeld, M. (2010): *X-Ray Spectrom.* 39, 103 – 111.

Corresponding author:
Matthias Alfeld (matthias.alfeld@gmx.de)